

Location and properties of respiratory neurones with putative intrinsic bursting properties in the rat *in situ*

Walter M. St.-John¹, Ruth L. Stornetta², Patrice G. Guyenet² and Julian F.R. Paton³

¹Department of Physiology, Dartmouth Medical School, Dartmouth-Hitchcock Medical Center, Lebanon, NH 03755 U.S.A.

²Department of Pharmacology, University of Virginia School of Medicine, Charlottesville, VA 22908 U.S.A.

³Department of Physiology and Pharmacology, Bristol Heart Institute, School of Medical Sciences, University of Bristol, Bristol BS8 1TD, UK

Using the *in situ* arterially perfused preparations of both neonatal and juvenile rats, we provide the first description of the location, morphology and transmitter content of a population of respiratory neurones that retains a bursting behaviour after ionotropic receptor blockade. All burster neurones exhibited an inspiratory discharge during eupnoeic respiration. These neurones were predominantly glutamatergic, and were located within a region of the ventral respiratory column that encompasses the pre-Bötzinger complex and the more caudally located ventral respiratory group. Bursting behaviour was both voltage and persistent sodium current dependent and could be stimulated by sodium cyanide to activate this persistent sodium current. The population of burster neurones may overlap with that previously described in the neonatal slice *in vitro*. Based upon the present and previous findings, we hypothesize that this burster discharge may be released when the brain is subject to severe hypoxia or ischaemia, and that this burster discharge could underlie gasping.

(Received 3 February 2009; accepted after revision 30 April 2009; first published online 5 May 2009)

Corresponding authors J. F. R. Paton: Department of Physiology & Pharmacology, School of Medical Sciences, University of Bristol, Bristol BS8 1TD, UK. Email: Julian.F.R.Paton@Bristol.ac.uk; W. M. St.-John: Department of Physiology, Dartmouth Medical School, Dartmouth-Hitchcock Medical Center, Lebanon, NH 03755 USA. Email: Walter.M.StJohn@Dartmouth.edu

Eupnoea and gasping are two patterns of automatic ventilatory activity which are generated by mechanisms that are intrinsic to the respiratory control system of pons and medulla. Under conditions of severe hypoxia or ischaemia, normal eupnoeic breathing ceases and is replaced by gasping (Lumsden, 1923, 1924; St.-John, 1990; Paton *et al.* 2006).

We have proposed that the switch from eupnoea to gasping represents a suppression of the pontomedullary neuronal circuit which is essential for generating eupnoea and a release of intrinsically bursting medullary neurones which generate gasping (St.-John, 1996; Paton *et al.* 2006; Paton & St.-John, 2007; Smith *et al.* 2007). This intrinsic bursting is dependent on conductances through persistent sodium channels (Paton *et al.* 2006). Supporting these concepts of different mechanisms generating eupnoea and gasping is the finding that gasping, but not eupnoea, is eliminated following administration of drugs that block conductances through persistent sodium channels (Paton *et al.* 2006; St.-John *et al.* 2007).

In previous studies using the *in situ* preparation of the juvenile rat, we have evaluated the hypothesis that medullary neuronal activities exhibiting discharge characteristics consonant for generating a gasp would

acquire a spontaneous, burster discharge following the blockade of fast synaptic transmission. Such a burster discharge was exhibited by a proportion of neuronal activities which had commenced their discharge just before or concomitant with the onset of the phrenic burst in eupnoea and gasping (Paton *et al.* 2006). These previous results represented the first demonstration of medullary burster neurones in a preparation other than *in vitro* preparations of neonatal rats (e.g. medullary slice or brainstem *en bloc*). However, our examination was limited to one region of the medulla and to one type of respiratory neuronal activity that had a discharge pattern consistent with generating the gasp. Hence, the question remains as to whether respiratory neurones with a potential intrinsic burster discharge represent a unique medullary population.

In the present studies, again using the *in situ* preparation of the juvenile rat, the uniqueness of the medullary respiratory burster population was defined based upon examination of multiple criteria as follows. (1) Anatomical region of the medulla. As opposed to *in vitro* slice preparations (Smith *et al.* 1991; Ramirez *et al.* 1996; Lieske *et al.* 2000), the *in situ* preparation used here has an intact pontomedullary brainstem. Thus, we

explored if neurones with a burster discharge were limited to the medullary pre-Bötzinger complex – the region explored *in vitro*- or were distributed in adjacent regions of the ventrolateral medulla. (2) Discharge pattern. We evaluated the hypothesis that neurones with a potential intrinsic burster discharge, manifested after a blockade of fast synaptic transmission, would represent a limited population. Hence, only a subpopulation of neurones having an inspiratory discharge pattern in eupnoea would be bursters. Most neurones with inspiratory, expiratory or phase-spanning activities in eupnoea would not become bursters. (3) Morphology of the burster neurones. We explored the axonal and dendritic projections of these neurones for comparison with those reported from the *in vitro* preparations; we were particularly interested to see if there was evidence of axonal projections to the contralateral ventrolateral medulla. (4) Synthesis and release of neurotransmitters. As inhibitory synaptic transmission is not essential for generating gasping (St.-John & Paton, 2002), we hypothesized that neurones with a burster discharge would be found to synthesize glutamate, as an excitatory neurotransmitter. (5) Basis for burster discharge. We examined the sensitivity of some burster neurones to blockade of persistent sodium current. This allowed us to determine whether burster activities were generated by mechanisms other than through the persistent sodium conductance; other conductances had been reported as essential for discharge of some types of burster cells *in vitro* (see Ramirez & Garcia, 2007 for review).

In addition to these studies using the juvenile rat preparation, we undertook studies to characterize changes in membrane potential of some neurones with a burster discharge during whole cell patch clamp recordings (Paton & St.-John, 2005). A perfused preparation of the neonatal rat was used. Neonatal, rather than juvenile, rats were used as the increased myelination of the older rats would decrease the probability of successful whole cell recordings. In this context, while it is recognized that both eupnoea and gasping may undergo some degree of maturation with age, yet both patterns, and differences between these, are quite similar in the neonate and juvenile rat (e.g. Wang *et al.* 1996).

Methods

Ethical approval

All surgical, experimental and euthanasia procedures conformed to the United Kingdom's Animals (Scientific Procedures) Act 1986 and were approved by the Ethics Committee of the University of Bristol. These procedures were also approved by the Institutional Animal Care and Use Committee of Dartmouth Medical School and Dartmouth College, USA.

General procedures

Perfused preparations of the juvenile (14–21 days of age, $n = 62$) and neonatal rat (6–8 days of age, $n = 27$) were used. These preparations were similar to that described originally in mouse (Paton, 1996) and identical to those described previously in rat (St.-John & Paton, 2000; Paton & St.-John, 2005; Paton *et al.* 2006). Under deep anaesthesia with halothane, the portion of the body caudal to the diaphragm was removed. The preparation was immersed in ice-cold mock cerebrospinal fluid and decerebrated at a precollicular level. In some preparations, a cerebellectomy was performed. Anaesthesia was discontinued.

The descending aorta was cannulated and artificial perfusion was commenced. The perfusate contained the following in distilled water (mM): MgSO_4 1.25, KH_2PO_4 1.25, KCl 3.0, NaHCO_3 24, NaCl 125, CaCl_2 2.5, dextrose 10, Ficoll 70 0.1785. Under control conditions, the perfusate was equilibrated with 95% O_2 –5% CO_2 . The temperature of the perfusate as it entered the aorta was $31 \pm 1^\circ\text{C}$. Efferent activity of the phrenic nerve was recorded with a suction electrode, amplified, filtered (0.6–6.0 kHz) and integrated (50 ms time constant).

In some preparations, a bipolar electrode was inserted into the spinal cord at an upper cervical level. The electrode was typically placed contralateral to the site of recording of respiratory neuronal activity in the medulla as most bulbo-spinal neurones have contralateral axonal projections (e.g. Saether *et al.* 1987). Stimuli (1 Hz; 0.2 ms, 0.1–10 V) were delivered through this electrode in an attempt to activate medullary neuronal activities by antidromic invasion. Criteria for antidromic invasion were as described previously (Bianchi & St.-John, 1985).

Whole cell patch clamp recordings in neonatal rat preparations

The patch pipettes and procedures of recording were as we have described previously in the perfused preparation (Paton & St.-John, 2005). Pipettes have a resistance of 4.0–5.5 $\text{M}\Omega$, as measured after filling with an intracellular solution and when placed within the tissue. This solution contained the following (mM): potassium gluconate 130, Hepes 10, EGTA 11, NaCl 4, MgCl_2 2, CaCl_2 1, ATP 2, GTP 0.5, glucose 5. The pH was 7.2 and the osmolarity was 290–300 mosmol l^{-1} .

Following identification of respiratory neurones within the ventrolateral medulla by extracellular recording using a low impedance glass microelectrode (1–3 $\text{M}\Omega$; Fig. 1Aa), pipettes were advanced into the same electrode track towards the ventrolateral medulla via a dorsal approach (Paton & St.-John, 2005). The electrodes and pipettes were held in a water hydraulic micro-manipulator (Narishige, Tokyo, Japan). Once the pipette was within the

ventrolateral medulla, extracellular spikes of neurones can usually be observed before the whole cell configuration is established. After establishing this configuration, recordings were made in bridge mode, with filtering at 3 kHz. Seal and access resistances were greater than 1.5 G Ω and 20–30 M Ω , respectively. After recording, pipettes were broken off above the dorsal surface of the medulla so as to be able to identify the recording site by the location of the tip of the pipette in subsequent histology (Fig. 1*Ab*). The

tissue was fixed in paraformaldehyde prior to sectioning (40 μ m thick).

Extracellular recordings of activities of single neurones in the juvenile rat

Activities of single neurones, having a discharge linked to the periods of activity and inactivity of the phrenic nerve, were recorded. Recordings of neuronal activities

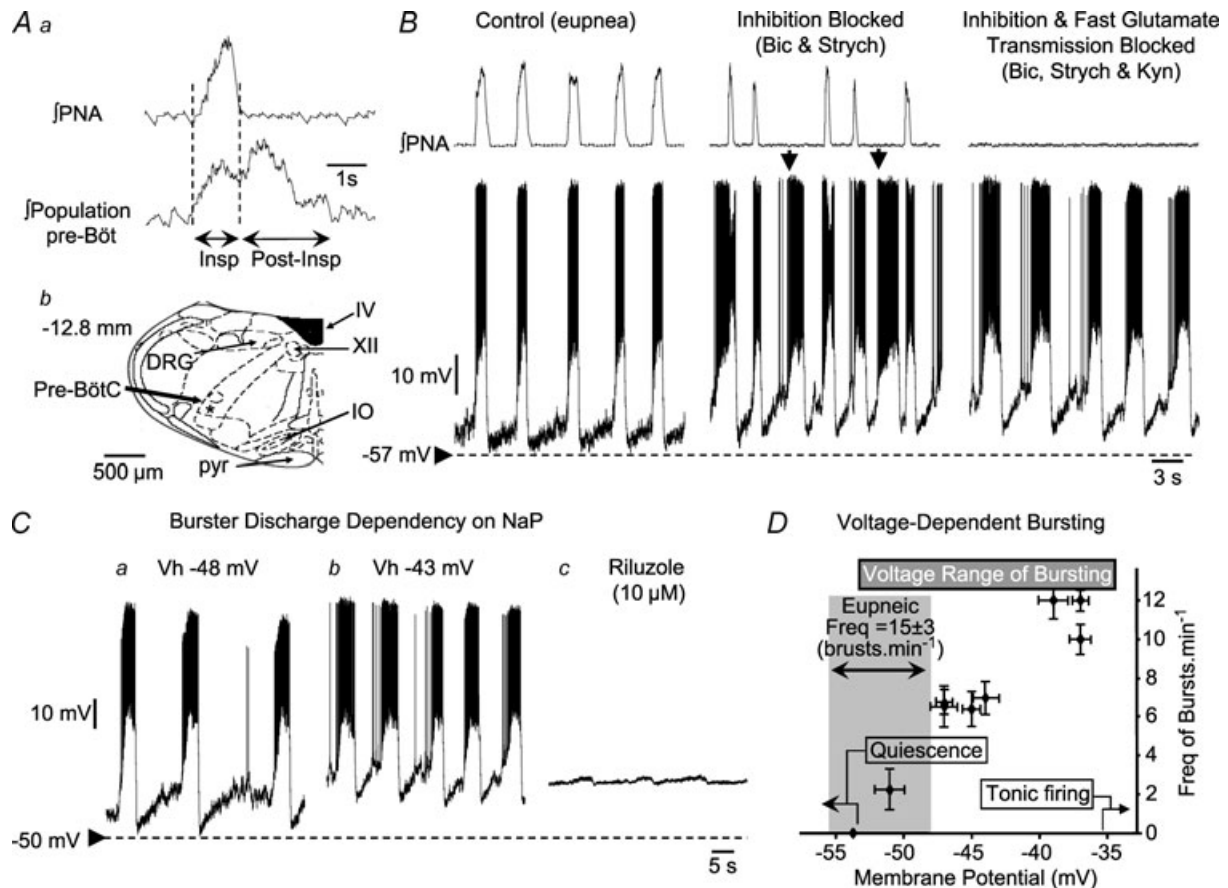


Figure 1. Example of discharges of burster neurones recorded intracellularly using patch pipettes from the ventral respiratory column

Prior to patch recording, low impedance microelectrodes were used to map the respiratory column (*A*). Once mapped, patch pipettes were placed into this region and recordings made from inspiratory neurones during eupnoea (*B*). Note that membrane potential depolarized during neural expiration, with the discharge phase-locked with the phrenic bursts (\int PNA; *B*). Following additions of bicuculline (Bicuc) and strychnine (Strych) to the perfusate (Inhibition Blocked; *B*), neuronal bursting showed some uncoupling from the phrenic burst (arrowed). Endogenous bursting was revealed on blocking both inhibitory and excitatory (Kynurenic acid, Kyn) fast synaptic transmission – Inhibition and Fast Glutamate Transmission Blocked. Note the absence of any phrenic discharge but phasic firing of medullary burster. The location of the recording site of this neurone was in the pre-Bötzing complex (*Ab*). There was a dependency of frequency of bursting upon membrane potential (*Ca* and *b* and *D*). Depolarization of neurones caused an increase in burst frequency (*Ca* and *b* and *D*). Note that burst frequency of this neurone did not match that seen during eupnoea even at the most depolarized levels. Bursting was eliminated following addition to the perfusate of 10 μ M of riluzole, a blocker of persistent sodium channels (*Cc*). Small oscillations in membrane potential after riluzole most probably represent an incomplete blockade of currents through persistent sodium channels. Abbreviations: DRG, dorsal respiratory group; IO, inferior olive; Pre-BötC, pre-Bötzing complex; pyr, pyramid; IV, fourth ventricle; XII, hypoglossal motor nucleus.

were made with glass pipettes that were filled with a solution of 1.5% biotinamide (Invitrogen, Paisley, UK; 15 mg ml⁻¹ in 0.5 M sodium acetate). The biotinamide was used for juxtacellular labelling of neurones, as described below. Microelectrodes were held in a 3-D micro-manipulator and advanced using a water hydraulic-driven system (Narishige). These microelectrodes were placed on the dorsal surface of the medulla and orientated using surface landmarks viewed through a binocular microscope. Signals were amplified, filtered (0.1–10 kHz) and recorded. The region examined was in the rostral medulla, including that approximating the rostral ventral respiratory column, the 'pre-Bötzinger and Bötzinger complexes' and the rostral ventral respiratory group.

Blockade of fast synaptic transmission in both neonatal and juvenile rats

To block excitatory synaptic transmission by glutamate, kynurenic acid was added to the perfusate in increments of 1 mM until phrenic discharge ceased. The quantity of kynurenic acid that was required varied greatly in different experiments (4–24 mM). To block inhibitory synaptic transmission at GABA_A receptors, bicuculline (20 μM) was added. Strychnine (1 μM) was used to block receptors for glycine. In some studies, bicuculline and strychnine were added before kynurenic acid. However, the sequence was reversed after we noted that, with the addition of kynurenic acid prior to bicuculline and strychnine, perfusion pressure remained constant. If the blockers of inhibitory synaptic transmission were added first, perfusion pressure increased markedly during the additions of kynurenic acid. This increase in perfusion pressure often resulted in the loss of recording of neuronal activity. The time required for the addition of all blockers was approximately 5 min. All blockers were from Sigma (Dorset, UK).

Verification of a blockade of fast synaptic activity followed criteria fully established previously (Paton, 1997; Paton *et al.* 2006). Most directly, in studies involving whole cell recordings (see above), this blockade of synaptic transmission was verified by an elimination of both spontaneous and evoked excitatory postsynaptic potentials; the latter were induced by electrical stimulation (1–10 V, 0.1 ms, 1 Hz) of the ipsilateral nucleus of the solitary tract. Additional criteria included the elimination of phrenic discharge and the absence of any recruitment of this phrenic discharge following stimulation of the carotid chemoreceptors by injection of sodium cyanide (6.1 mM, 0.1 ml) into the aorta via a side port from the perfusion system. Finally, bicuculline and strychnine at the concentrations that we used normally cause seizure-like discharge. Adding these antagonists after kynurenic acid was a potent test to establish whether

excitatory transmission had been effectively blocked to prevent appearance of seizure discharge. In some cases, the blockers of inhibitory synaptic transmission re-activated phrenic (sometimes as a classical seizure discharge), but the latter was eliminated completely with further doses of kynurenic acid. This elimination of phrenic discharge was, we believe, a robust test validating the blockade of excitatory transmission.

Juxtacellular labelling of neurones in juvenile rats

Procedures were identical to those described previously (Schreihofer & Guyenet, 1997; Schreihofer *et al.* 1999). Recordings of neuronal activities were made with glass pipettes, filled with biotinamide as noted above. The tips of these microelectrodes were broken back to produce an impedance ranging from 15 to 30 MΩ when measured in 0.9% saline. At the termination of an experiment, following the blockade of fast synaptic transmission, neurones were filled with biotinamide, via anodal pulses of current (50% duty cycle, 400 ms pulse, 2.5 Hz, 0.5 to 8 nA). Current pulses were delivered for a minimum of 30 s and a maximum of 10 min.

At the end of the experiment, preparations were perfused with 150 ml of 4% paraformaldehyde. Brains were removed and stored in the same fixative solution prior to further processing.

In studies in which neurones were labelled with biotinamide, histology was performed in order to fulfil three aims. First, the precise anatomical location of the neurone was established. Second, the morphology of the burster neurones was characterized and compared with the morphology of neurones which became silent or discharged tonically following the blockade of fast synaptic transmission. In cases with adequate labelling, we documented axonal projections. Finally, we determined if these neurones were glutamatergic (Stornetta *et al.* 2003b).

Experimental protocol

With whole cell patch clamp, activities were recorded during eupnoea in the neonatal preparations. These recordings continued during stimulation of ventilatory activity by intra-arterial injections of sodium cyanide (see above). Drugs were then administered to block fast synaptic transmission. As noted above, in some studies, bicuculline and strychnine were administered prior to kynurenic acid and in others, this sequence was the reverse. After all drugs were given, the efficacy of the blockade was tested as described above. Recordings continued after this blockade and burster activities, if any, were characterized in response to injections of current to change membrane potential. In some trials, excitation was increased by the addition of potassium chloride (final concentration

7–11 mM) or sodium cyanide (9.0–15 μ M) to the perfusate. Riluzole (1–10 μ M) Sigma (Dorset, UK) was added to block conductance through persistent sodium channels. In previous studies (Paton *et al.* 2006), we have found that riluzole, or other blockers of conductance through persistent sodium channels, eliminated the discharge of every burster neurone on which it was tested.

In the juvenile preparations, extracellular recordings of neuronal activities were obtained in eupnoea. Again, blockers of fast synaptic transmission were administered and, following this blockade, neuronal activities were characterized as to burster discharge, if any. For such burster activities, this characterization included an attempt to establish axonal projections to the spinal cord, by antidromic invasion. The burster discharge was also characterized in response to augmentations in excitation by administrations of potassium chloride or sodium cyanide. It is well recognized that sodium cyanide, through the production of hypoxia of tissues, increases conductance through persistent sodium channels, which is essential for burster discharge (e.g. Hammarstrom & Gage, 1998; Koizumi & Smith, 2008). Thus, 10-fold higher concentrations relative to those used to activate carotid bodies were infused to activate persistent sodium channels. In some cases, we recorded pairs of rhythmically active units through the same microelectrode. To demonstrate that these cells were synaptically isolated from each other, we performed cross correlation analysis (Spike 2, Cambridge Electronic Design, Cambridge, UK).

Neurones were then entrained with current pulses (see above) with the intention of labelling with biotinamide. Some neurones that failed to acquire a burster discharge were also labelled.

In some preparations and following the blockade of fast synaptic transmission, we searched for burster activities at identical coordinates in the contralateral medulla and, if found, characterized this burster discharge and entrained these neurones with the aim of labelling these neurones with biotinamide.

Statistical evaluations were by Student's *t* test for paired or unpaired data. Values are expressed as mean \pm S.E.M.

Results

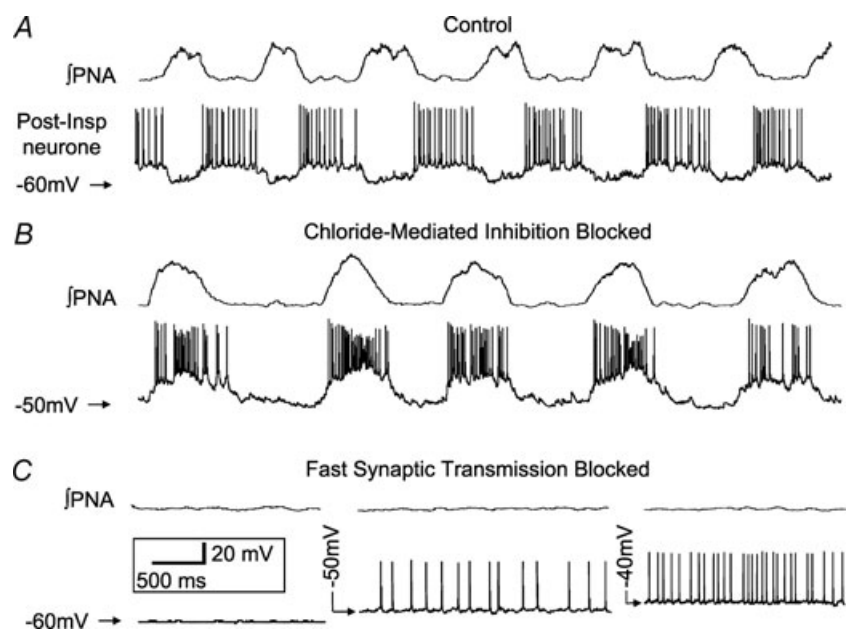
Respiratory neuronal activities were sought in the rostro-ventrolateral medulla. Electrodes for whole cell or extracellular recordings were inserted into the brainstem just rostral to the rostral-most edge of the area postrema, which was visible on the medullary surface. Activities which were taken for recording were 1.6 to 3.0 mm below the dorsal surface of the brainstem. We did not conduct a systematic search of this region as our aim was to characterize activities of neurones which might acquire a burster discharge rather than cataloguing the various types of medullary respiratory neuronal activities in a region.

Whole cell recordings of burster activities in the neonatal rat

Activities of twenty-seven neurones were recorded during the sequence of eupnoea and the blockade of synaptic transmission. Twenty-two of these neurones had inspiratory (Fig. 1) or expiratory–inspiratory discharge patterns with the others having an expiratory discharge (Fig. 2). All neurones generated spikes that were >50 mV

Figure 2. Representative example of an expiratory neurone that did not exhibit intrinsic bursting after blockade of fast synaptic transmission

This whole cell recording of a post-inspiratory neurone showed inspiratory mediated hyperpolarisation in control conditions (A) but after blockade of fast chloride mediated synaptic inhibition exhibited inspiratory related depolarization and burst discharge (B). The latter reported previously by us (Büsselberg *et al.* 2001; Dutschmann & Paton 2002) indicates the presence of inspiratory-related glutamatergic drive that is shunted out by synaptic inhibition under control conditions. Subsequent blockade of glutamatergic ionotropic transmission resulted in a loss of phrenic nerve activity (PNA) and tonic firing at resting membrane potential (-50 mV; C). Despite manoeuvring membrane potential this neurone failed to generate intrinsic bursting.



in amplitude. There was no significant difference in membrane potential (measured during their inactivity) for inspiratory and expiratory neurones (-53 ± 2 versus -54 ± 5 mV respectively; $P = 0.6$). Neurones had input resistances ranging from 55 to 350 M Ω (mean = 135 ± 45 M Ω). Following the administrations of bicuculline, strychnine and kynurenic acid, all expiratory and seventeen of the inspiratory/expiratory–inspiratory neuronal activities ceased or discharge tonically (Fig. 2). In all cases altering their membrane potential (depolarize/hyperpolarize) failed to induce bursting but the frequency of tonic activity was altered (Fig. 2C). The remaining five neurones acquired a burster discharge (Fig. 1). Membrane input resistance was not significantly different between bursters and non-bursters ($P > 0.1$).

Activities of two representative burster neurones are shown in Fig. 1. In Fig. 1B, the activity of the neurone and phrenic nerve are shown in eupnoea and following the blockade of fast synaptic activity. Following administrations of bicuculline and strychnine alone, the neurone had periodic discharges that were independent of the phrenic bursts (Fig. 1B arrowed). Following administrations of kynurenic acid, the neurones continued spontaneous membrane depolarizations and bursts of activity. For this and the other burster activities, the frequency of bursting was dependent upon the membrane potential and increased with depolarizations

(Fig. 1C). The voltage range over which bursting occurred spontaneously was between -51 ± 2 mV to -37 ± 2 mV ($n = 5$); more hyperpolarized potentials resulted in quiescence and more depolarized potentials cause tonic firing (Fig. 1D). During eupnoeic respiration, burster neurones had a membrane potential of -55 ± 1 mV (expiratory phase) and fired consistently with the phrenic discharge at a mean frequency of 15.3 ± 3 bursts min^{-1} ($n = 5$). Following blockade of fast synaptic transmission, maximal burst frequency evoked at the most depolarized potential was 12.1 ± 2 bursts min^{-1} ($n = 5$) and not significantly different from their firing frequency during eupnoea ($P > 0.2$). However, at the membrane potential we measured prior to synaptic blockade (i.e. -55 ± 1 mV), bursters were quiescent and below the voltage threshold for intrinsic burst generation (Fig. 1D). Also, as for all burster activities that were recorded, the burster discharge was eliminated following administrations of riluzole (Fig. 1C), a blocker of persistent sodium currents, as described by us previously (Paton *et al.* 2006).

This neuronal activity depicted in Fig. 1 was located in the region of the pre-Bötzinger complex of the medulla (Fig. 1Ab). As described below in detail other neuronal activities were in this region or in the region of the rostral ventral medullary respiratory nucleus.

Figure 3 shows a verification of synaptic blockade for an inspiratory neuronal activity. Prior to the blockade

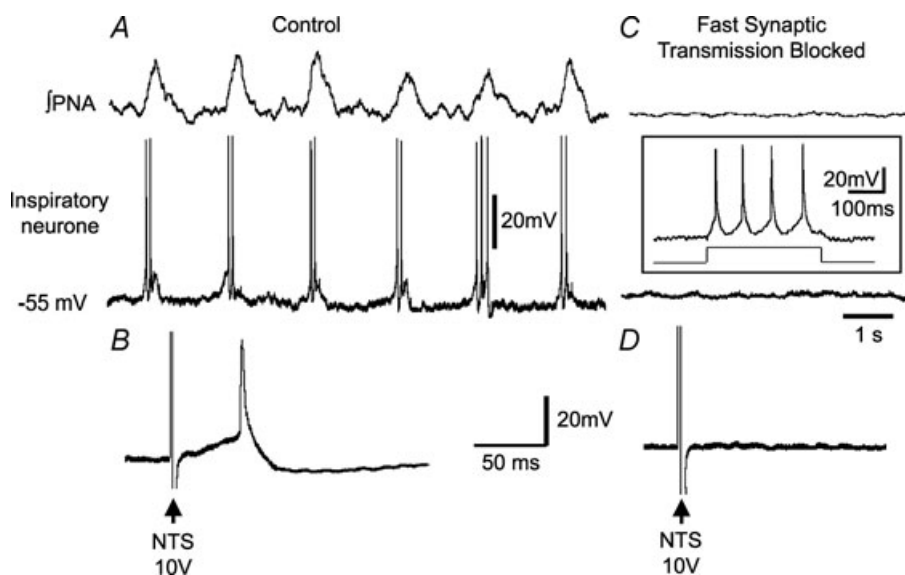
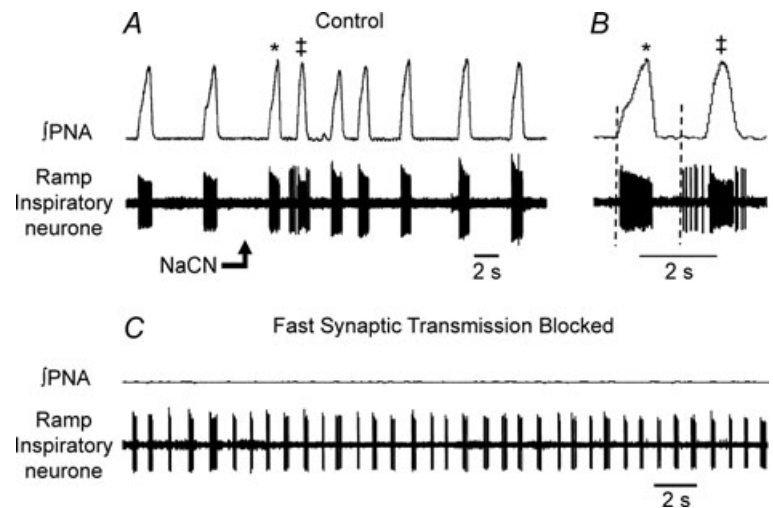


Figure 3. Verification of blockade of synaptic transmission by elimination of excitatory postsynaptic potentials induced by stimulation of the nucleus tractus solitarii (NTS)

Control panel (A) shows integrated activity of the phrenic nerve (*f* PNA) and an intracellular recording of activity of a neurone having an inspiratory discharge pattern. B shows excitatory postsynaptic potential and spike evoked by stimulation of the nucleus tractus solitarii. Variables of stimulation were single pulses of 0.2 ms duration. In C fast inhibitory and excitatory synaptic activity had been blocked by addition of the 'cocktail' of bicuculline, strychnine and kynurenic acid (see Methods). Note the elimination of the phrenic discharge and both spontaneous activity and depolarization of the neurone. The inset shows that depolarization of the neurone by injection of 200 pA current resulted in generation of action potentials, indicating that the intracellular recording was being maintained. However, stimulation of the nucleus tractus solitarii no longer elicited a depolarization/spike (D), confirming blockade of fast synaptic transmission.

Figure 4. Release of medullary burster activity following a blockade of fast synaptic transmission

Control recordings (A) are of integrated activity of the phrenic nerve (\int PNA) and of activity of a single medullary ramp inspiratory neurone. Peripheral chemoreceptors were stimulated by an intra-arterial bolus injection of sodium cyanide (NaCN; 50 μ l, 0.03%): note the pre-inspiratory discharge evoked in this neurone (B). * and ‡ indicated the bursts prior to and during the chemoreceptor reflex-evoked response; the burst labelled ‡ exhibits the pre-inspiratory discharge. In C, bicuculline, strychnine and kynurenic acid (8.0 mM) were added to the perfusate to block inhibitory synaptic transmission at GABA_A receptors, at receptors for glycine, and ionotropic glutamate receptors respectively. Phrenic discharge ceased and burster discharges commenced. No increase in extracellular potassium was required to evoke this activity which persisted for the duration of the recording (>20 min).



during eupnoea, the neurone exhibited a spike at a short latency following electrical stimulation of the nucleus tractus solitarii (Fig. 3B). Following the blockade, the spontaneous discharge of the neurone ceased, as did all subthreshold postsynaptic activity, although injection of current could evoke a series of action potentials (Fig. 3C). However, no action potentials followed stimulation of the nucleus tractus solitarii, thus verifying the blockade of synaptic transmission at the intracellular level (Fig. 3D).

Extracellular recordings in juvenile rats

Activities of 66 inspiratory-related medullary neurones were recorded prior to, and following the blockade of fast synaptic transmission. In addition, the activities of 15 neurones were recorded from the same region on

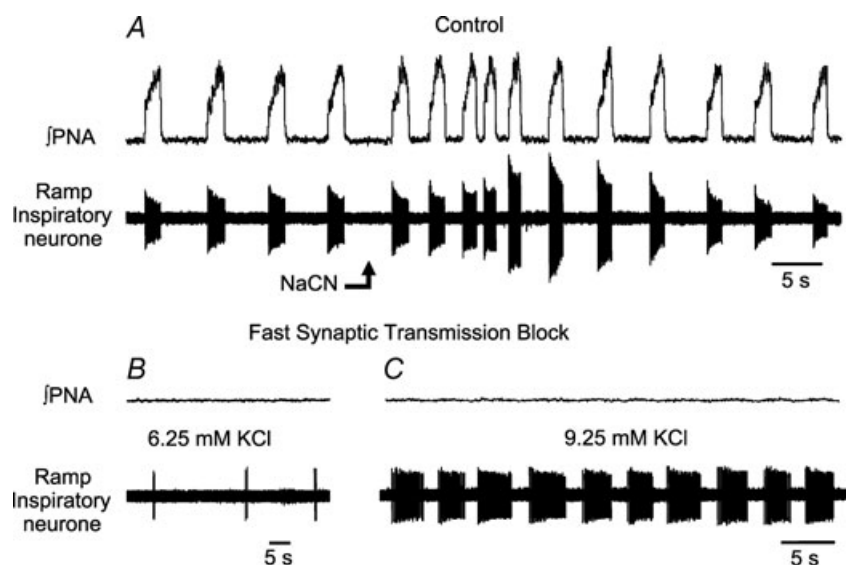
the contralateral side following this blockade. Hence, activities of this latter group of 15 neurones could not be characterized based on their phase of firing relative to phrenic activity.

Prior to the blockade of fast synaptic transmission, all neuronal activities had phasic discharge patterns that either commenced prior to and during the period of the phrenic burst or coincided with the onset of the phrenic burst (Figs 4 and 5). For eight of these 66 neuronal activities, the discharge commenced in the mid to late portions of neural expiration.

Pharmacological stimulation of the carotid chemoreceptors by intracarotid injections of sodium cyanide caused augmentations in the frequency and amplitude of phrenic discharge and in the frequency of neuronal discharges within a latency of less than 1 s (Figs 4 and 5). In some neurones, extra bursts of neuronal activity

Figure 5. Influence of elevations of concentration of potassium chloride upon discharge of a medullary burster neurone

A, control recordings are of integrated activity of the phrenic nerve (\int PNA) and activity of a single medullary ramp inspiratory neurone. This cell was activated by peripheral chemoreceptor stimulation with a bolus injection of sodium cyanide (NaCN; 50 μ l, 0.03%). Note that change in spike height of neurone was due to a small movement of the brainstem following the injection. Following additions of bicuculline, strychnine and kynurenic acid (16.0 mM) to the perfusate, phrenic discharge was eliminated (B). Weak bursts of neuronal activity were observed after the addition of 2.0 mM KCl (total = 6.25 mM) (B), but were greatly augmented by addition of a further 3.0 mM of KCl to the perfusate (total = 9.25 mM) (C). Note, phrenic nerve activity remained blocked (C).



were observed in the period between phrenic bursts, or the onset of firing of the neurone occurred earlier relative to the onset of phrenic activity (e.g. Fig. 4A and B). However, such changes following sodium cyanide were not consistently observed in all neurones characterized subsequently as bursters (Fig. 5). Indeed, non-burster neuronal activities could also show similar responses following activation of peripheral chemoreceptors.

Following additions of kynurenic acid to the perfusate, the frequency and peak height of phrenic discharge declined to a cessation of activity (Figs 4 and 5). Additions of bicuculline and strychnine caused a modest return of phrenic discharge in some trials but, following an increment in the concentration of kynurenic acid, this discharge was eliminated. Likewise eliminated was the rhythmic discharge of 52 neuronal activities. Of the remaining 14, three discharged tonically with a periodic and repetitive increase in discharge frequency. Six neuronal activities were spontaneously phasic and another five neurones acquired a phasic discharge following augmentations in the concentration of potassium chloride in the perfusate (Fig. 5). None of the neurones that acquired a burster discharge following the blockade of fast synaptic transmission was antidromically activated by stimulation of the spinal cord.

Following the blockade of fast synaptic transmission, there was no seeming relationship between the frequency of neuronal bursts and the frequency of phrenic bursts during eupnoea before the blockade of synaptic transmission. This lack of relationship was consistent with that found in whole cell recordings (see above; Fig. 1D). For approximately 60% of the neurones, the frequency of bursts was lower following the blockade of fast synaptic transmission and for the other 40%, the frequency was higher. For all trials, there was no significant difference between phrenic discharge in eupnoea ($16.6 \pm 2.3 \text{ min}^{-1}$) and the neuronal discharge following blockade of fast synaptic transmission ($10.3 \pm 1.3 \text{ min}^{-1}$; $P > 0.1$) the latter number includes neurones which did or did not require augmentations in the concentration of KCl for bursting to be manifested.

Following a blockade of fast synaptic transmission, the short latency augmentation in neuronal activity by intra-carotid administration of sodium cyanide was eliminated. However, as shown in Fig. 6, additions of relatively high concentrations of sodium cyanide to the perfusate (see Methods) caused an elicitation of burster discharge with a marked augmentation in the frequency of this discharge and its intra-burst firing frequency. Such high concentrations of sodium cyanide were given in previous studies to augment the persistent sodium conductance (Hammarstrom & Gage, 1998; Koizumi & Smith, 2008).

Following the complete blockade of fast synaptic transmission and elimination of phrenic discharge, neuronal activities were sought in the same region on the contralateral side. A total of 15 bursters were found with a mean discharge frequency of $16.2 \pm 3.5 \text{ min}^{-1}$, which was not different from the frequency of bursters described above ($P > 0.17$). The discharge pattern of the bursters was heterogeneous, as shown by the examples of these burster activities in Fig. 7. However, long duration bursts were typically decrementing (Fig. 7Da). Such heterogeneity was the same as that observed for activities of burster neurones that were recorded continuously before and after the blockade of fast synaptic transmission.

Figure 7C shows recording following the blockade of fast synaptic transmission in which multiple burster discharges were recorded simultaneously, through the same electrode. To assess if these neurones had 'pauci-synaptic' connections, we performed cross correlation analysis ($n = 3$ pairs). No significant correlations were found, which strongly implies that these neurones were synaptically isolated. Also, note that these neurones exhibited very different frequencies of their bursting. A similar heterogeneity in burster discharge was also seen with whole cell recordings (e.g. Fig. 1). Thus, the relatively homogeneous inspiratory or expiratory–inspiratory discharges in eupnoea became heterogeneous following the blockade of fast synaptic transmission. Again, none of these burster neurones that were tested showed evidence of antidromic invasion following stimulation of the spinal cord.

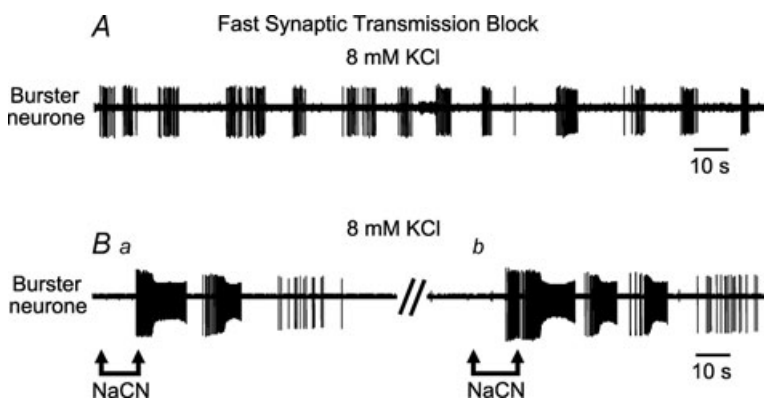


Figure 6. Elicitation of bursting by infusions of sodium cyanide

A shows activity of a burster neurone recorded after a block of fast synaptic transmission and after raising extracellular potassium to 8 mM. This unit was not characterised during eupnoea but located after blockade of synaptic transmission. The burster activity was somewhat irregular but could be repeatedly excited by intra-arterial infusions of sodium cyanide (NaCN 0.03%) to the perfusate (B). Ba shows a response after 9.0 μM NaCN and Bb after addition of 12 μM NaCN.

Juxtacellular labelling of neurones in the juvenile rat preparation

Figure 7*Db* shows the entrainment of a neuronal activity by electrical stimulation to eject biotinamide iontophoretically. Initially the intensity of the pulses of positive current (50% duty cycle, 400 ms; see Methods) was raised until the discharge of the neurone was entrained. Current could then be reduced to approximately 1–5 nA, and entrainment continued for 30 s to 10 min. Spike activity was monitored continuously to be certain that activity of another neurone was not recruited by the current pulse stimulation.

Forty-four single neuronal activities were entrained *in situ* (only one neurone per side of the brainstem) and 32 biotinamide-labelled neurones were recovered after histological processing. This success rate (73%) is comparable to what is typically achieved with conventional anaesthetized rat preparations (Schreihofer *et al.* 1999; Stornetta *et al.* 2003*a,b*). Of the 32 recovered neurones, 19 had exhibited a burster discharge following the blockade of synaptic transmission; the other 13 had become silent. In the working heart–brain pre-

paration, juxtacellular labelling of a single cell also leads to extensive deposition of biotinamide in the capillaries that surround the targeted neurone (Fig. 8). Reasons for this artifact remain unclear but it limited our ability to reconstruct the dendritic structure of the labelled neurones to a few cases in which the neurone was labelled exceptionally well. One example of a burster neurone is shown in Fig. 8. This neurone had a small, fusiform cell body. It was located in the pre-Bötzinger region and its axon extended beyond the midline towards the contralateral side. This cell contained a low level of vesicular glutamate transporter 2 mRNA reaction product (VGLUT2) and was presumably glutamatergic. Other examples of biotinamide-labelled glutamatergic burster neurones are also shown in Fig. 8*C*, illustrating the range of intensities of the VGLUT2 mRNA reaction product detected in the labelled burster neurones. The biotinamide-labelled neurones (burstlers and non-burstlers) were located within an approximate 700 μm rostrocaudal stretch of the ventral respiratory column that was centred at the level of the area postrema (Fig. 9). The anatomical distribution of burstlers and non-burstlers was the same and there was no

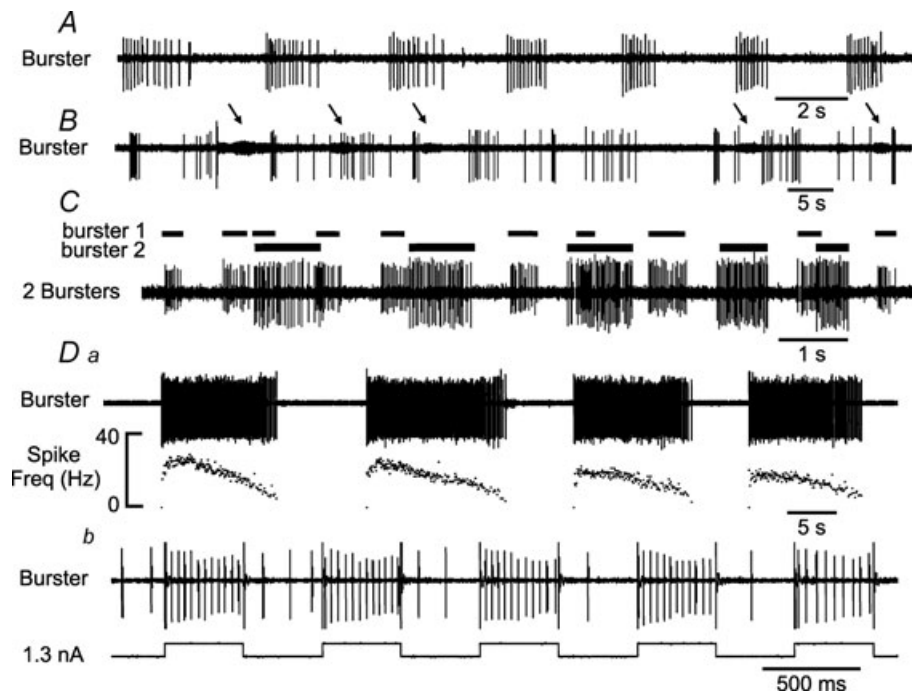


Figure 7. Examples of discharge of three burster neurones recorded from the medulla following a blockade of fast synaptic transmission

Note the different frequencies of discharge of the three burster neurones (A–D). In B, there is a second burster in the background (arrowed). In C, two bursters were recorded simultaneously from a single microelectrode; note their different firing rates and patterns indicating that synaptic transmission was blocked. Horizontal bars indicate the duration of the bursts of each neurone. In Da, the firing pattern was of a decrementing type, a typical feature of medullary burstlers with long discharge duration. In detail, the initial period of neuronal discharge was very steeply augmenting, followed by a brief plateau and then a rate of decline that was much slower than the initial rate of rise. The neurone was entrained by applying current pulses in an attempt to label the neurone juxtacellularly by iontophoretic injection of biotinamide (Db).

obvious difference in their soma shape (see Fig. 8). Dorsal landmarks are unreliable to identify precisely the rostro-caudal location of neurones located within the ventrolateral medulla because of variations in the angle of cut of the sections. The location of the neurones was therefore identified in relation to ventral medullary structures such as the caudal end of the facial motor nucleus, the lateral reticular nucleus and the nucleus ambiguus.

Only a small minority of the bursters (4/19) were recovered in the region that corresponds to the classically defined pre-Bötzinger complex. This segment of the ventral respiratory column is thought to reside medial to

the nucleus linearis below the caudal end of the compact division of nucleus ambiguus and rostral to the two distinctive rostral horns of the lateral reticular nucleus (Fig. 9, level 630). The rest of the bursters were found caudal to this level, i.e. between the two horns of the lateral reticular nucleus or caudal to this level above the lateral reticular nucleus (levels 890 and 1070 in Fig. 9). This level corresponds to the classically described rostral ventral respiratory group.

Seventy-four percent of the bursters (14/19) and 54% of the non-bursters (7/13) were VGLUT2-positive and therefore presumably glutamatergic. These percentages

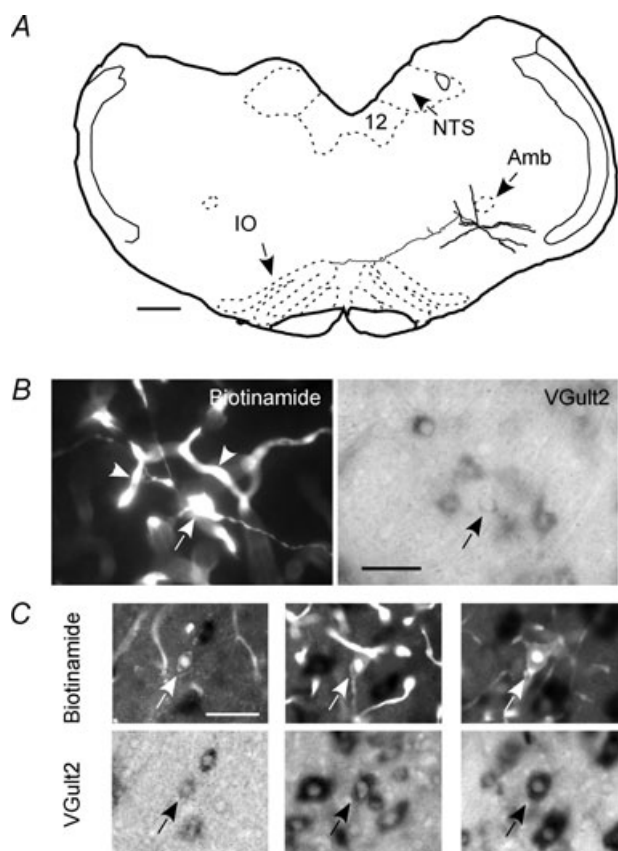


Figure 8. Examples of glutamatergic inspiratory neurones
 A shows the structure of an inspiratory burster. This neurone was located within the pre-Bötzinger region of the ventral respiratory column (VRC) just below the caudal end of the nucleus ambiguus, pars compacta (Amb). Its axon had local collaterals within the ipsilateral VRC and projected past the midline in a roughly coronal plane (IO, inferior olive; NTS, nucleus of the solitary tract; 12, hypoglossal nucleus). Scale 0.5 mm. B shows photomicrographs of the burster neurone shown in A. Its cell body (arrow) and proximal dendrites are shown in the left panel (biotinamide revealed with Alexa 488 fluorescence). Many capillaries located in the vicinity of the labelled neurone also contain biotinamide (arrowheads). The right panel shows the reaction product for VGLUT2 mRNA. Scale 50 μm . C shows three additional examples of 'intrinsic' bursters to illustrate the range of intensity of the VGLUT2 mRNA reaction product observed in these cells (top panels: biotinamide; bottom panels: VGLUT2 mRNA). Scale for all C panels: 50 μm .

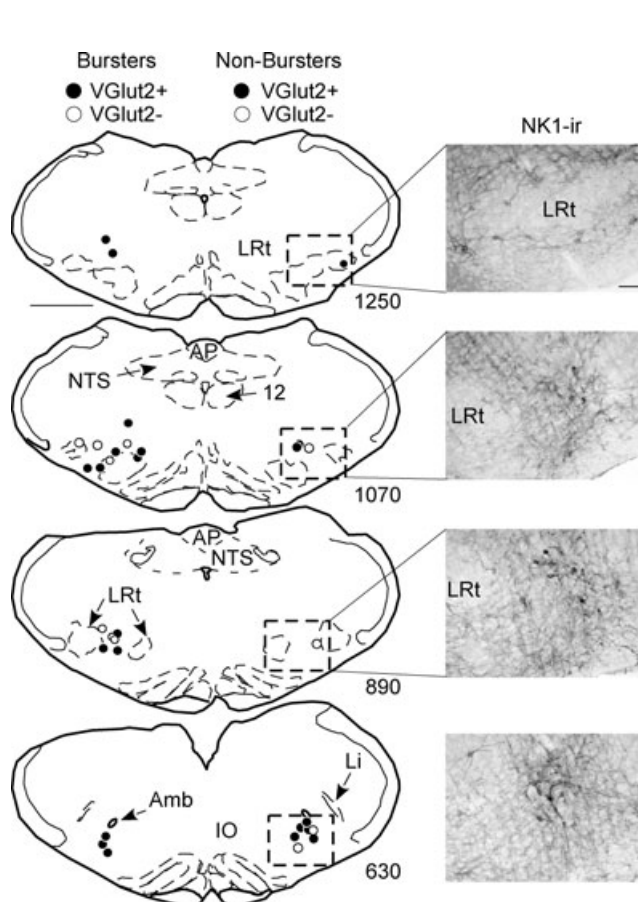


Figure 9. The location of all biotinamide-labelled inspiratory neurones is plotted on four standardized coronal sections through the medulla oblongata (scale bar: 500 μm)
 The bursters are plotted on the left and the non-bursters on the right. The numbers at the lower right of the sections indicate the observed distance between the section and the caudal end of the facial motor nucleus in micrometres. Due to the small brain size of the juvenile rat, these distances are smaller than that published in existing atlases of rat brains. The photographs located at the right of the standardized sections represent immunoreactivity for the NK1 receptor within the region represented by the boxes. NK1 reactivity was examined in three rats of the same size as the experimental subjects (calibration 100 μm). Amb, nucleus ambiguus, pars compacta; AP, area postrema; Li, nucleus linearis; LRt, lateral reticular nucleus; NTS, nucleus of the solitary tract; 12: hypoglossal nucleus.

could be underestimated owing to variations in the quality of the detection of VGLUT2mRNA.

Discussion

In this study, we provide the first description of the location, morphology and transmitter content of a population of respiratory neurones that retains a bursting behaviour after blockade of ionotropic receptors in neonatal and juvenile rats *in situ*. Burster neurones were generally glutamatergic and were located in a region spanning the pre-Bötzinger complex and the rostral ventral respiratory group. Before synaptic blockade, the burster neurones were invariably inspiratory and these cells initiated their phasic firing either coincident with phrenic activity or prior to it (i.e. pre-inspiratory phase). We conclude that the anatomical distribution and properties of the bursters in the *in situ* preparation have many similarities with the *in vitro* slices of neonate medulla oblongata (Johnson *et al.* 1994).

Evidence for intrinsic bursters

We considered as 'intrinsic bursters' those neurones that discharged spontaneously with series of action potentials after administrations of kynurenic acid, bicuculline and strychnine. These drugs would not have blocked all synaptic transmission within the brainstem. Among others, ionotropic cholinergic transmission, metabotropic glutamate transmission and the serotonergic system would remain. Yet, in terms of the brainstem respiratory control system, our results strongly support the conclusion that 'intrinsic bursters' were synaptically isolated and their burster discharge was indeed 'intrinsic'. Evidence in support of this synaptic blockade is multiple. First, following administrations of kynurenic acid, bicuculline and strychnine, phrenic discharge ceased and could not be recruited in response to stimulation of the carotid chemoreceptors by sodium cyanide. In a related finding, following this blockade of synaptic transmission, synaptic potentials and action potentials that had been recruited by stimulations of the nucleus tractus solitarii were eliminated. A third piece of evidence for synaptic isolation was that the frequency of discharge of the 'intrinsic burster' neurones increased with electrical depolarizations. Contrariwise, some 'intrinsic bursters' were silent, with no evidence of subthreshold depolarizations, until levels of potassium chloride were increased to depolarize the neurones. The heterogeneous frequency of bursts recorded from different neurones is additional evidence for their synaptic isolation as any residual connectivity would have synchronized discharges. Following the blockade, discernable cells recorded simultaneously exhibited distinct burst frequencies (Fig. 7C).

Inherent to these considerations is the conclusion that burster activities recorded in neonatal preparations with patch pipettes and those recorded extracellularly in juvenile preparations were drawn from the same population. In support of this conclusion, we note that both groups of bursters had similar discharge frequencies, albeit heterogeneously distributed. In addition, although the size of the brainstems differed between neonatal and juvenile rats, burster activities in both were recorded from the same medullary regions, based upon histological evaluations.

The above evidence is consistent with that for activities of burster neurones recorded from *in vitro* medullary slices. Hence, as the 'intrinsic bursters' characterized herein, bursters of *in vitro* preparations were driven by an activator of persistent sodium current, such as sodium cyanide, and arrested by riluzole, an antagonist of channels mediating the persistent sodium current. Also, as the burster activities recorded in this study, those of *in vitro* slice preparations showed a voltage-dependent burst frequency (Smith *et al.* 1991; Butera *et al.* 1999a; Koizumi *et al.* 2008). Finally, the morphology of one of the 'intrinsic' burster neurones that happened to reside in the pre-Bötzinger complex was similar to that reported from *in vitro* studies (e.g. Koizumi *et al.* 2008). Notable resemblances included the location below the compact division of nucleus ambiguus and an axon that crossed the midline in a coronal plane, suggesting that it may have innervated neurones of the contralateral pre-Bötzinger complex and ventrolateral medulla. Similar axonal projections of 'pre-inspiratory' neurones of the pre-Bötzinger complex have been noted by others (Schwarzacher *et al.* 1995; Koshiya & Smith, 1999; Stornetta *et al.* 2003a,b). However, the majority of the bursters recorded in juvenile rats in the present experiments were not located in the region typically described as the pre-Bötzinger complex but were located caudal to that level, i.e. within the rostral portion of the ventral respiratory group (Alheid & McCrimmon, 2008). With one exception, regions caudal to the pre-Bötzinger complex have not been explored in detail in neonatal *in vitro* preparations from the standpoint of endogenous bursters. However, Johnson *et al.* (1994) provided clear evidence that respiratory neurones that retain bursting properties under conditions of reduced synaptic activity in medullary slices of neonates are virtually all inspiratory and that these cells are located both in the pre-Bötzinger complex and in the adjacent rostral ventral respiratory group (e.g. Johnson *et al.* 1994). This study in medullary slices is therefore in excellent agreement with our findings in the juvenile rat *in situ*.

One possible interpretation of both the present study and that of Johnson *et al.* (1994) is that inspiratory premotor neurones, which are abundant in the rostral portion of the ventral respiratory group also have latent

intrinsic bursting properties. Although this hypothesis is consistent with the fact that inspiratory premotor neurones are VGLUT2-positive (Stornetta *et al.* 2003b), our attempts at antidromic activation failed to reveal that the burster neurones had spinally projecting axons. This negative evidence is not conclusive, however, because we did not test every neurone for antidromic invasion and we did not positively identify any bulbospinal neurones with inspiratory discharges during our experiments. Accordingly, the present evidence does not exclude the possibility that the bursters that we have identified are a mixed population that may include pre-Bötzinger complex interneurones and inspiratory, potentially bulbospinal, premotor neurones. The latter may provide direct access of endogenous medullary inspiratory bursters to corresponding spinal motoneurones.

Hypothesized functional roles of medullary respiratory burster neurones in gasping and eupnoea

We hypothesize that the discharge of respiratory medullary bursters underlies gasping. The hypothesis is based upon the findings that processes that alter conductance through persistent sodium channels, which is essential for burster discharge, also alter the discharges of cranial and spinal nerves in gasping (Paton *et al.* 2006; Paton & St.-John, 2007). A seeming direct link between burster discharge and gasping is the elimination of both following administrations of riluzole, a blocker of conductances through persistent sodium channels (Paton *et al.* 2006; St.-John *et al.* 2007; St.-John, 2008). Equally the discharge of respiratory medullary bursters/persistent sodium current can be recruited for rebound burst generation after a period of hyperpolarisation, burst termination, regenerative excitation, breathing during sleep and embryological development of the brainstem respiratory network, for example (McKay *et al.* 2005; Thoby-Brisson *et al.* 2005; Koizumi & Smith, 2008). In addition, synchronization of population activity is also a plausible functional role of burster activity. This is consistent with our morphological evidence that points to a possible mechanism of synchronization in that burster neurones typically have axons which remain within the brainstem and can cross the midline. Given that burster discharges are desynchronized following a blockade of fast synaptic transmission, by administration of blockers of receptors for glutamate, GABA and glycine, it would seem probable that one or more of these neurotransmitters is responsible for the synchronization among bursters. Glutamate is the most probable candidate because it is considered as critical for synchronization of discharge among inspiratory neuronal activities of *in vitro en bloc* preparations (Ballanyi *et al.* 1999). Further evidence in support of the possibility that neurotransmission via glutamate might be critical for synchronization

among burster neurones is the present finding that almost 75% were positive for vesicular glutamate transporter 2 (VGLUT2). This percentage could be an underestimation due to the variable quality of the histological material, but it may also suggest that the population of bursters is heterogeneous. For example, a large number of pre-Bötzinger neurones are glycinergic (A.P.L. Abdala, J.C. Smith & J. F. R. Paton, unpublished observation). Whether the VGLUT-2 negative burster neurones described herein are glycinergic remains to be determined.

What is the intrinsic bursting behaviour of medullary burster neurones in eupnoea?

Although their intrinsic properties for endogenous bursting may not be active, it is clear that burster neurones are phasically firing coincidentally and exclusively with phrenic activity during eupnoea. In eupnoea, burster neurones exhibit a pattern of discharge that characterizes them as inspiratory or pre-inspiratory, as defined by membrane potential depolarization and/or firing ahead of the onset of phrenic activity in the late expiratory phase. From our experience, burster neurones could not be identified before blocking fast synaptic transmission as they failed to exhibit a consistent, characterizing phenotype. Indeed, their reflex response to peripheral chemoreceptor activation was again not specific allowing *a priori* characterization of a burster neurone.

We found that blockade of fast chloride mediated synaptic inhibition, prior to administration of kynurenic acid, caused ectopic discharge of subsequently characterized bursters. This ectopic discharge was a characteristic specific to bursters as it was never seen in cells that did not show phasic discharge after subsequent blockade of ionotropic glutamate transmission. Based on this evidence it follows that the intrinsic bursting behaviour is kept 'in check' by chloride-mediated synaptic inhibition in the intact eupnoeic network. We argue that the intrinsic burster property of these neurones is not needed for the generation of eupnoea. Rather, their firing is controlled by powerful reciprocating inhibitory connections (e.g. Richter & Spyer, 2001; Rybak *et al.* 2003; Smith *et al.* 2007). However, we do not rule out the possibility that current mediated through persistent sodium channels may contribute to burst pattern formation in eupnoea (Butera *et al.* 1999a,b) but it is unlikely to generate the eupnoeic rhythm.

Conclusions

The region of the ventral respiratory column that encompasses the pre-Bötzinger complex and the rostral ventral respiratory group contains inspiratory neurones that retain a bursting behaviour after blockade of fast

synaptic transmission in the neonatal and juvenile rat. Most of those cells are glutamatergic. They are presumably propriobulbar interneurons, but the possibility that a subset of these cells are premotor neurons was not eliminated by the present experiments. The ability of these inspiratory cells to burst after ionotropic receptor blockade relies in part on intrinsic properties because their burst frequency was increased by depolarizing current and their bursting was prevented by riluzole. This population of inspiratory neurons may include the mature form of the inspiratory bursters first identified in the neonatal pre-Bötzinger complex in slices.

References

- Alheid GF & McCrimmon DR (2008). The chemical neuroanatomy of breathing. *Respir Physiol Neurobiol* **164**, 3–11.
- Ballanyi K, Onimaru H & Homma I (1999). Respiratory network function in the isolated brainstem-spinal cord of newborn rats. *Prog Neurobiol* **59**, 583–634.
- Bianchi AL & St.-John WM (1985). Changes in antidromic latencies of medullary respiratory neurones in hypercapnia and hypoxia. *J Appl Physiol* **59**, 1208–1213.
- Büsselberg, D, Bischoff, AM, Paton, JFR & Richter, DW (2001). Loss of glycinergic inhibition reveals two modes of respiratory rhythm generation. *Pflügers Archiv* **441**, 444–449.
- Butera RJ, Rinzel J & Smith JA (1999a). Models of respiratory rhythm generation in the pre-Bötzinger complex. I. Bursting pacemaker neurones. *J Neurophysiol* **82**, 382–397.
- Butera RJ, Rinzel J & Smith JA (1999b). Models of respiratory rhythm generation in the pre-Bötzinger complex. II. Populations of coupled pacemaker neurones. *J Neurophysiol* **82**, 398–415.
- Dutschmann M & Paton JFR (2002). Glycinergic inhibition is essential for co-ordinating cranial and spinal respiratory motor outputs in the neonatal rat. *J Physiol* **543**, 643–653.
- Hammarstrom AK & Gage PW (1998). Inhibition of oxidative metabolism increases persistent sodium current in rat CA1 hippocampal neurones. *J Physiol* **510**, 735–741.
- Johnson SM, Smith JC, Funk GD & Feldman JL (1994). Pacemaker behaviour of respiratory neurones in medullary slices from neonatal rat. *J Neurophysiol* **72**, 2598–2608.
- Koizumi H & Smith JC (2008). Persistent Na⁺ and K⁺-dominated leak currents contribute to respiratory rhythm generation in the pre-Bötzinger complex *in vitro*. *J Neurosci* **28**, 1773–1785.
- Koizumi H, Wilson CG, Wong S, Yamanishi T, Koshiya N & Smith JC (2008). Functional imaging, spatial reconstruction, and biophysical analysis of a respiratory motor circuit isolated *in vitro*. *J Neurosci* **28**, 2353–2365.
- Koshiya N & Smith JC (1999). Neuronal pacemaker for breathing visualized *in vitro*. *Nature* **400**, 360–363.
- Lieske SP, Thoby-Brisson M, Telgkamp P, Ramirez J-M (2000). Reconfiguration of the neural network controlling multiple breathing patterns: eupnea, signs and gasps. *Nat Neurosci* **3**, 600–607.
- Lumsden T (1923). Observations on the respiratory centres in the cat. *J Physiol* **57**, 153–160.
- Lumsden T (1924). Effects of bulbar anaemia on respiratory movements. *J Physiol* **59**, lvii–lx.
- McKay LC, Janczewski WA & Feldman JL (2005). Sleep-disordered breathing after targeted ablation of pre-Bötzinger complex neurones. *Nat Neurosci* **8**, 1142–1144.
- Paton JFR (1996). The ventral medullary respiratory network of the mature mouse studied in a working heart-brainstem preparation. *J Physiol* **493**, 819–831.
- Paton JFR (1997). Rhythmic bursting of pre- and post-inspiratory neurones during central apnoea in mature mice. *J Physiol* **502**, 623–639.
- Paton JFR, Abdala APL, Koizumi H, Smith JC & St.-John WM (2006). Respiratory rhythm generation during gasping depends on persistent sodium current. *Nat Neurosci* **9**, 311–316.
- Paton JFR & St.-John WM (2005). Long-term intracellular recordings of respiratory neuronal activities during eupnea and gasping *in situ*. *J Neurosci Methods* **147**, 138–145.
- Paton JFR & St.-John WM (2007). Medullary pacemakers are essential for the neurogenesis of gasping, but not eupnea. *J Appl Physiol* **103**, 718–722.
- Ramirez JM & Garcia A (2007). Medullary pacemaker neurones are essential for both eupnea and gasping in mammals. *J Appl Physiol* **103**, 717–718.
- Ramirez JM, Quellmalz UJA & Richter DW (1996). Postnatal changes in the mammalian respiratory network as revealed by the transverse brainstem slice preparation of mice. *J Physiol* **491**, 799–812.
- Richter DW & Spyer KM (2001). Studying rhythmogenesis of breathing: comparison of *in vivo* and *in vitro* models. *Trends Neurosci* **24**, 464–472.
- Rybak IA, Shevtsova NA, St.-John WM, Paton JFR & Pierrefiche O (2003). Endogenous rhythm generation in the pre-Bötzinger complex and ionic currents: modelling and *in vitro* studies. *Eur J Neurosci* **18**, 239–257.
- Saether K, Hilaire G & Monteau R (1987). Dorsal and ventral respiratory groups of neurons in the medulla of the rat. *Brain Res.* **419**, 87–96.
- Schreihofer AM & Guyenet PG (1997). Identification of C1 presympathetic neurones in rat rostral ventrolateral medulla by juxtacellular labelling *in vivo*. *J Comp Neurol* **387**, 524–536.
- Schreihofer AM, Stornetta RL & Guyenet PG (1999). Evidence for glycinergic respiratory neurones: Bötzing neurones express mRNA for glycinergic transporter 2. *J Comp Neurol* **407**, 583–597.
- Schwarzacher SW, Smith JC & Richter DW (1995). Pre-Bötzinger complex in the cat. *J Neurophysiol* **73**, 1452–1461.
- Smith JC, Abdala APL, Koizumi H, Rybak IA & Paton JFR (2007). Spatial and functional architecture of the mammalian brain stem respiratory network: a hierarchy of three oscillatory mechanisms. *J Neurophysiol* **98**, 3370–3387.
- Smith JC, Ellenberger HH, Ballanyi K, Richter DW & Feldman JL (1991). Pre-Bötzinger complex: a brainstem region that may generate respiratory rhythm in mammals. *Science* **254**, 726–729.

- St.-John WM (1990). Neurogenesis, control and functional significance of gasping. *J Appl Physiol* **68**, 1305–1315.
- St.-John WM (1996). Medullary regions for neurogenesis of gasping: noeud vital or noeuds vitals? *J Appl Physiol* **81**, 1865–1877.
- St.-John WM (2008). Eupnea of *in situ* rats persists following blockers of *in vitro* pacemaker burster activities. *Respir Physiol Neurobiol* **160**, 353–356.
- St.-John WM & Paton JFR (2000). Characterizations of eupnea, apneusis and gasping in a perfused rat preparation. *Respir Physiol* **123**, 201–213.
- St.-John WM & Paton JFR (2002). Neurogenesis of gasping does not require inhibitory transmission using GABA_A or glycine receptors. *Respir Physiol Neurobiol* **132**, 265–277.
- St.-John WM, Waki H, Dutschmann M & Paton JFR (2007). Maintenance of eupnea of *in situ* and *in vivo* rats following riluzole, a blocker of persistent sodium channels. *Respir Physiol Neurobiol* **155**, 97–100.
- Stornetta RL, Rosin DL, Wang H, Sevigny CP, Weston MC & Guyenet PG (2003a). A group of glutamatergic interneurons expressing high levels of both neurokinin-1 receptors and somatostatin identifies the region of the pre-Bötzinger complex. *J Comp Neurol* **455**, 499–512.
- Stornetta RL, Sevigny CP & Guyenet PG (2003b). Inspiratory augmenting bulbospinal neurons express both glutamatergic and enkephalinergic phenotypes. *J Comp Neurol* **455**, 113–124.
- Thoby-Brisson M, Trinh JB, Champagnat J & Fortin G (2005). Emergence of the pre-Bötzinger respiratory rhythm generator in the mouse embryo. *J Neurosci* **25**, 4307–4318.
- Wang W, Fung ML, Darnall RA & St.-John WM (1996). Characterizations and comparisons of eupnea and gasping in neonatal rats. *J Physiol* **490**, 277–292.

Author contributions

Each of the authors contributed to all aspects of these studies, from formulation of the hypotheses, to conducting the experiments and writing the manuscript. The neurophysiological investigations were performed by W.M.St.-J. and J.F.R.P. at both the University of Bristol and Dartmouth Medical School. The neurohistochemical evaluations were performed at the University of Virginia by R.L.S. and P.G.G.

Acknowledgements

This work was supported by grants 26091 and 74011 from the National Heart, Lung and Blood Institute, National Institutes of Health (USA). J.F.R.P. was in receipt of a Royal Society Research Merit Award.